Sun
Terrestrial, Atmospheric and Oceanic Sciences (2024) 35:2
https://doi.org/10.1007/s44195-024-00060-y

Terrestrial, Atmospheric and Oceanic Sciences

ORIGINAL ARTICLE

Open Access

An efficient forward semi-Lagrangian model

Wen-Yih Sun[1,2*]

Abstract

An efficient forward trajectory model is proposed, in which the property and position of the fluids advected from the Euler coordinates to the Lagrangian coordinates can be accurately evaluated. After sorting and aligning those fluid elements on the irregular Lagrangian curves, we apply the cubic or other high-degree polynomials to interpolate the properties of the elements from the irregular curves to the regular grids. There is no need to solve the cubic equations and the associated coefficients as proposed previously. The model is quite simple, accurate, and much more efficient than the previous models. It also allows higher-order polynomials to be employed in the interpolations. It is suitable for simulating the multi-dimensional fast-moving flows with large Courant Numbers, the transport of pollutants in the atmosphere and ocean, and movement of raindrops in atmospheric models.

Keywords Lagrangian scheme, Semi-Lagrangian, Forward, Backward, Courant number, Courant–Friedrichs–Lewy criterion (CFL), Euler and Lagrangian coordinates

1 Introduction

The characteristic-based Lagrangian models have been successfully applied to simulate the vortex merging, hydraulic jumps, and shear flows in the shallow water equations (Toro 1999; Wang and Yeh 2005, and others) with CFL ≥ 1, their results are quite accurate compared with the high-order finite volume models (Sun 2011; Sun and Oh 2022), but the former requires tremendous computing time. They are also difficult to apply to multi-dimensional flows. Hence, the semi-Lagrangian advections are popular in computational fluid dynamics (Staniforth and Cote 1991). It is noted that there is a big challenge to find the property of the fluid in the upstream regions in fluid dynamics (Kalnay et al 2000; Fournier 2005; Sun and Sun 2017). The conventional backward schemes may face similar challenges. On the other hand, the forward trajectory method can easily evaluate the fluid property in the downstream with great accuracy (Purser and Leslie 1991). However, the variables on a curvilinear Lagrangian grid are difficult to evaluate in the equations. Purser and Leslie (1991) proposed the 'cascade interpolation method', which was also used in Nair et al. (2003) and others. Sun et al. (1996) proposed the 'split interpolation method'. Based on splitting the dimensions of the geometric space to simplify the interpolation formulae, both methods are very efficient with satisfactory accuracy. Because both methods hypothesize the same coordinate monotonicity, they are also subject to the restriction that neither the x- nor the y-projections of the Lagrangian curves should cross, which may not require CFL ≤ 1, but is still more stringent than the stability criterion of Sun and Yeh (1997) semi-Lagrangian scheme. It is noted that the numerical scheme applied to the flux-form model also requires CFL ≤ 1. A numerical scheme that allows CFL much greater than unity can be useful to simulate the fast-moving, high deformation flows inside hurricanes (Kurihara et al. 1998) and tornados (Fujita 1974, 1992), along the upper-level jet or the low-level jet, and strong vertical updrafts and downdraft inside the hot towers in the Equator trough (Rielh and Malkus 1958; Sun 2023), and the high-speed raindrop falling in the sky and the downslope density current (Setter and Kuo 1983; Sun 1993); or to ease the CFL constraint imposed by the unwanted acoustic waves in a compressible fluid

*Correspondence:
Wen-Yih Sun
wysun@purdue.edu
[1] Department of Earth, Atmospheric, and Planetary Sciences, Purdue University, West Lafayette, IN 47906, USA
[2] Department of Atmospheric Sciences, National Central University, Taoyuan 320317, Taiwan

and/or gravity waves in the Quasi-geostrophic phenomena (Sun and Sun 2015, 2019; Yeh et al. 2002). Because of high accuracy and simplicity, the current scheme is suitable to simulate the long-distance transport of dust by the upper-level-jet (Sun et al. 2013) and dispersion of pollution over the complex terrain (Wu et al. 2003; Sun 2021).

Sun and Yeh (1997) (will be referred to as SY) proposed a direct projection from the regular grids to the irregular Lagrangian grids in the 2D flow with velocity (u, v). Figure 1 shows that the fluid from the grid O(ξ, η) on $\eta = y_j$ moves to P(X,Y).(indicated by red circle) on the Lagrangian curve $\eta = y_j$ within Δt, where X = ξ + uΔt, and Y = η + vΔt. The variable *F* (for example, water substance or pollutant) and the Lagrangian coordinates of the parcel remain the same, although the location changes from $O(\xi, \eta)$ to *P(X,Y)* in Euler coordinates. They:

(A) Arranged the data in an orderly sequence,
(B) Assumed that variables *F* and the coordinate of *P(X,Y)* on the Lagrangian curve $\eta = y_j$, are given by the cubic polynomials of ξ:

$$X(\xi) = a_3\xi^3 + a_2\xi^2 + a_1\xi + a_0, \tag{1a}$$

$$Y(\xi) = b_3\xi^3 + b_2\xi^2 + b_1\xi + b_0, \tag{1b}$$

$$F(\xi) = c_3\xi^3 + c_2\xi^2 + c_1\xi + c_0. \tag{1c}$$

Used 4-points values of ξ on $\eta = y_j$ and at *P(X,Y)* to determine the coefficients of a_k, b_k, and c_k in the section of $d\xi = \xi_{j+1} - \xi_j$, where *P(X,Y)* is located.

(C) If the curve of $\eta = y_j$ intercepting the vertical line at $X = X_k$, as indicated by the blue diamond Q in Fig. 1, they solved and selected the appropriate $\xi_{X_k,j}$ among three roots of

$$a_3\xi^3 + a_2\xi^2 + a_1\xi + a_0 = X_k. \tag{1d}$$

Then, put $\xi_{X_k,j}$ in Eqs. (1b) and (1c) to obtain the *Y* and *F* at Q; and applied same method to other Lagrangian curves to obtain entire interceptions of blue diamonds (Qs) on vertical line at $X = X_k$.

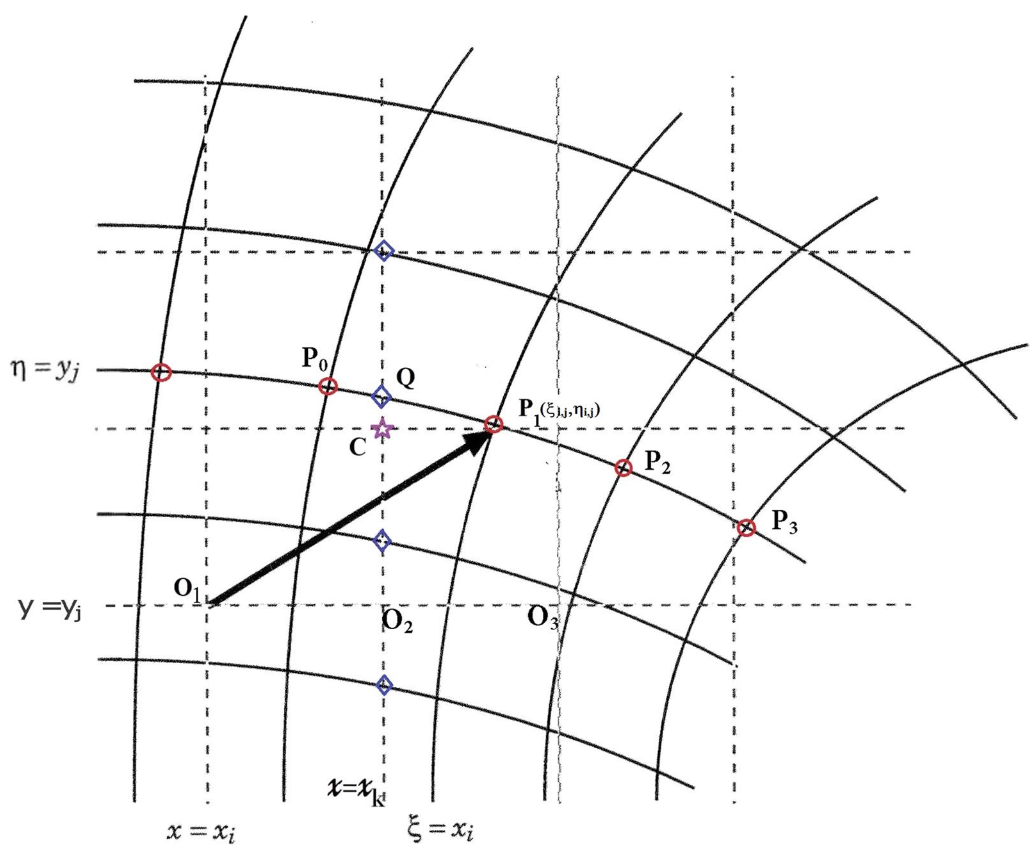

Fig. 1 A particle O in Euler grids (dashed lines) moves to P in Lagrangian grids (full lines), and the corresponding Eulerian coordinate lines x = xi and y = yj are transformed to the Lagrangian coordinate lines ξij and ηij, respectively

(D) From the values and y-coordinates of (Qs) along the vertical line to derive the value at the regular grid C (purple star in Fig. 1), then repeated the same procedure for the grids in the entire domain

This method is as accurate as Purser and Leslie (1994), Nair et al. (2003) or Sun et al. (1996). It is not limited by the restriction of coordinate monotonicity, either. Hence, it can be applied to the flow with CFL > 1. Although it requires 1.7 to 2.3 times computation compared with the splitting method, it is still more efficient than the backward semi-Lagrangian scheme according to SY. The SY scheme has been applied in a 3D nonhydrostatic model to simulate the flows over mountains, and convective cloud bands develop over a warm ocean (Hsieh et al. 2010; Hsu et al. 2004, etc.) SY also showed solving coefficients of Eqs. (1a, 1b, 1c) and the roots of cubic Eq. (1d) consume most of their computing resources. Meanwhile, equations higher than the third degree are exceedingly difficult to solve, hence, they cannot be applied in SY.

Here, we propose a method that requires solving neither the coefficients nor the cubic equations. The new method not only significantly reduces the procedures, saving 2/3 or more of computing time, but also allows higher-order polynomials to be employed. To compare with SY results, we will show the simulations using the 3rd-order polynomials in the flow with large Courant Numbers.

2 Numerical scheme

As described previously, the fluid moves from $O_i(\xi,\eta)$ to $P_i(X,Y)$(indicated by red circle) within Δt in the regular coordinates. We connect those red circles to form the Lagrangian curve (η = yj), which intercepts with the vertical line at X = Xk, indicated as blue diamond point Q. Since the variables on the Lagrangian curve are related to the cubic polynomials of the Lagrangian coordinates of the parcels, ξ and η, they can also be represented by the cubic polynomials of X and Y, the Euler coordinates of the parcels, because X and Y are well-defined functions of ξ and η. Consequently, $F(X_k)$ and $Y(X_k)$ can be derived from the coordinates of the neighboring reds by the Lagrangian polynomials:

$$\begin{aligned}F(X) =& F_{i-2,j}\frac{(X-X_{i-1,j})(X-X_{i,j})(X-X_{i+1,j})}{(X_{i-2,j}-X_{i-1,j})(X_{i-2,j}-X_{i,j})(X_{i-2,j}-X_{i+1,j})}\\ &+F_{i-1,j}\frac{(X-X_{i-2,j})(X-X_{i,j})(X-X_{i+1,j})}{(X_{i-1,j}-X_{i-2,j})(X_{i-1,j}-X_{i,j})(X_{i-2,j}-X_{i+1,j})}\\ &+F_{i,j}\frac{(X-X_{i-2,j})(X-X_{i-1,j})(X-X_{i+1,j})}{(X_{i,j}-X_{i-2,j})(X_{i,j}-X_{i-1,j})(X_{i,j}-X_{i+1,j})}\\ &+F_{i+1,j}\frac{(X-X_{i-2,j})(X-X_{i-1,j})(X-X_{i,j})}{(X_{i+1,j}-X_{i-2,j})(X_{i+1,j}-X_{i-1,j})(X_{i+1,j}-X_{i,j})}\end{aligned} \tag{2a}$$

$$\begin{aligned}Y(X) =& Y_{i-2,j}\frac{(X-X_{i-1,j})(X-X_{i,j})(X-X_{i+1,j})}{(X_{i-2,j}-X_{i-1,j})(X_{i-2,j}-X_{i,j})(X_{i-2,j}-X_{i+1,j})}\\ &+Y_{i-1,j}\frac{(X-X_{i-2,j})(X-X_{i,j})(X-X_{i+1,j})}{(X_{i-1,j}-X_{i-2,j})(X_{i-1,j}-X_{i,j})(X_{i-2,j}-X_{i+1,j})}\\ &+Y_{i,j}\frac{(X-X_{i-2,j})(X-X_{i-1,j})(X-X_{i+1,j})}{(X_{i,j}-X_{i-2,j})(X_{i,j}-X_{i-1,j})(X_{i,j}-X_{i+1,j})}\\ &+Y_{i+1,j}\frac{(X-X_{i-2,j})(X-X_{i-1,j})(X-X_{i,j})}{(X_{i+1,j}-X_{i-2,j})(X_{i+1,j}-X_{i-1,j})(X_{i+1,j}-X_{i,j})}\end{aligned} \tag{2b}$$

After obtaining *F* and *Y* of all intercepts (blue diamonds) on the vertical line at $X = X_k$, we apply Eq. (2a) again but on the vertical direction by replacing X by Y to get the value *F* at the Euler grid C. The same procedure is applied to the entire domain. There is no need to solve the cubic equations or the associated coefficients. Hence, this scheme is much simpler and more efficient than the one proposed by SY. It is noted that following the same procedure, the vertical Lagrangian curves can be interpolated from the fluids initially coming from the vertical lines, ξ_i. Interpolation from the Lagrangian curves projected by fluids coming from either a horizontal or vertical curve to the regular grids is referred to as 'Economic Internet Interpolation.' On the other hand, interpolation using both vertical and horizontal lines parcels came from is called 'Complete Internet Interpolation' (SY). They showed that Complete Interpolation is slightly more accurate than Economic Interpolation, but the Complete version requires twice computing resources as the Economic one. It is also noted that Eq. (2a, 2b) used in this model can be replaced by the 5th or higher order polynomials here, but not in SY.

3 Numerical results of Doswell's idealized cyclogenesis

The idealized cyclogenesis of Doswell (1984) is used to demonstrate the performance of the scheme applied to a rotational flow with strong deformation. The governing equation is

$$\frac{\partial f}{\partial t} = -\mathbf{V}\cdot\nabla f \text{ in Euler forms, or } \frac{Df}{Dt} = 0 \text{ in Lagrangian form.} \tag{3a}$$

The tangential velocity of the circular vortex is.

$$V(r) = A\,\mathrm{sech}^2(r)\tanh(r), \tag{3b}$$

where *r* is the radius of the vortex; A = 2.598 is chosen so that the maximum value of *V* equals 1. The initial condition is.

$$f(x,y,0) = -\tanh[(y-y_c)/\delta], \tag{3c}$$

where δ is the characteristic width of the frontal zone, as defined in in Holm (1995). The analytic solution is.

$$f(x,y,t) = -\tanh\left[\frac{(y-y_c)}{\delta}\cos(\omega t) - \frac{(x-x_c)}{\delta}\sin(\omega t)\right] \tag{3d}$$

where $(x_{c,}\ y_c)$ is the center of rotation and $\omega = V/r$ is the angular velocity. The integration domain is 10 units long with resolutions of 65×65 or 129×129 grid points. An integration time of 5 units is chosen so that the analytic solution is still resolvable on the low-resolution grid. Nearly perfect results are obtained for the smooth cases with $\delta = 1$, and we are interested only in the non-smooth cases with $\delta = 0.05$. The analytic solution on the high-resolution grid is shown in Fig. 2a. The simulation from SY's Complete Version with the filters (Sun and Sun 2004; Sun 2007) on 129×129 grids, 64-time steps, t = 5, CFL = 1, and Error = 0.083 shown in Fig. 2b is quite comparable with our Economic simulation (Error = 0.078) in Fig. 2c. They are also in good agreement with our numerical result with 16-time steps, CFL = 4, t = 5, and Error = 0.076 in Fig. 2d. The numerical result obtained from SY's Complete Internet on 65×65 grids with CFL = 4, t = 5 and Error = 0.068 is shown in Fig. 3a. Our Economic simulation shown in Fig. 3b has Error = 0.147. A larger error indicates that twice of the data used in Complete Interpolation does improve the numerical results when the sharp edge of the vortex sheet is barely resolved by the coarse grids. When the phenomena can be well represented by the Lagrangian polynomials, the results do not have significant difference between our simple (Economic) model and SY's Complete Model. Both models can handle flows with the Courant Number much larger than one. The simulation on 129×129 grids with CFL = 6.0 produces an Error = 0.132 at t = 9.843, 21-time steps (shown in Fig. 4). The Error = 0.073 at t = 5.15 at 11-time steps. The mass

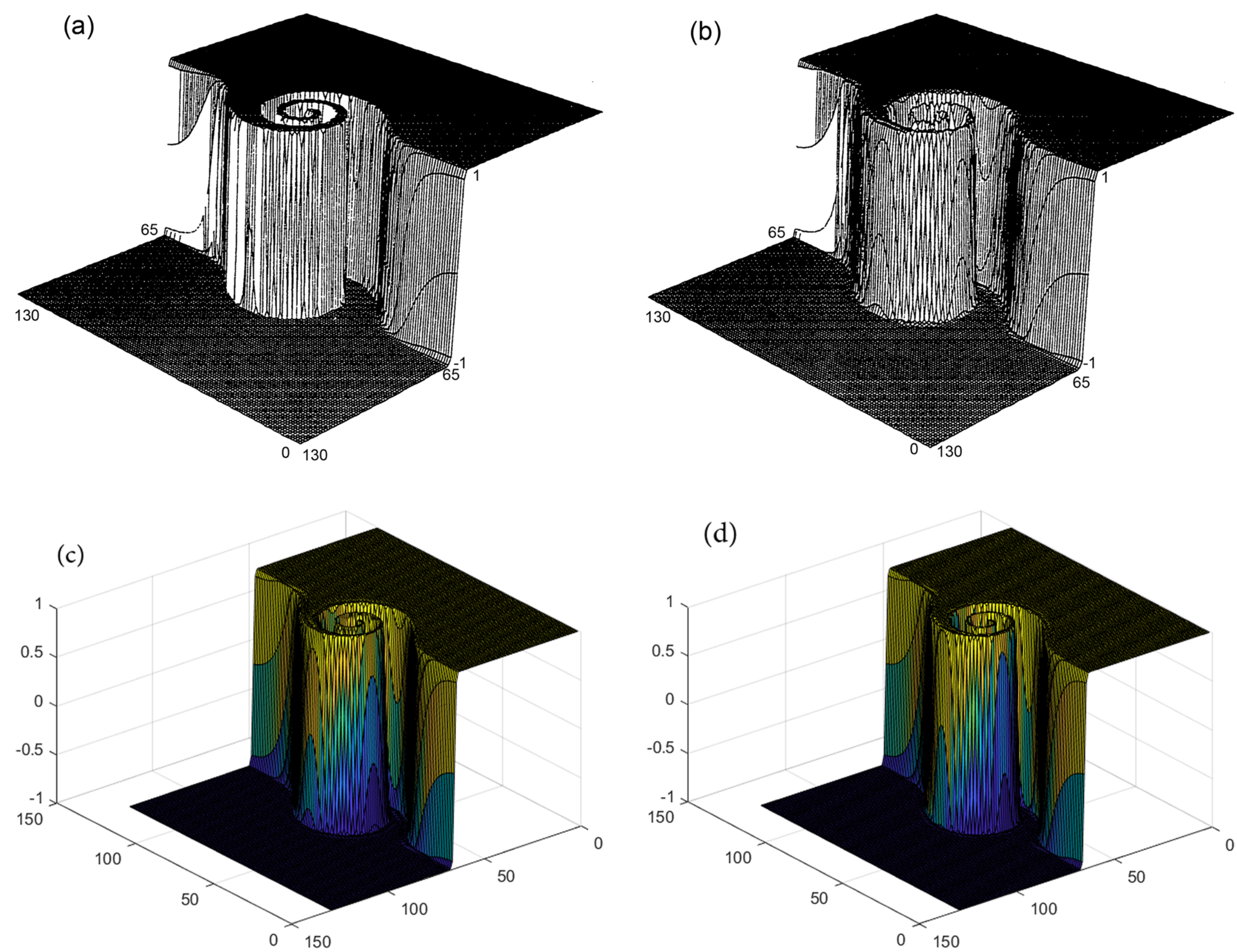

Fig. 2 The Idealized cyclogenesis test on 129×129 grids, $\delta = 0.05$. **a** The analytic solution after 5-time units: **b** simulation at the same time from Complete Internet of SY (64 time-steps, CFL = 1, Error = 0.083). **c** Simulation from current Model (64 time-steps, CFL = 1, Error = 0.078), **d** simulation from current model with 16 time-steps (CFL = 4, Error = 0.076)

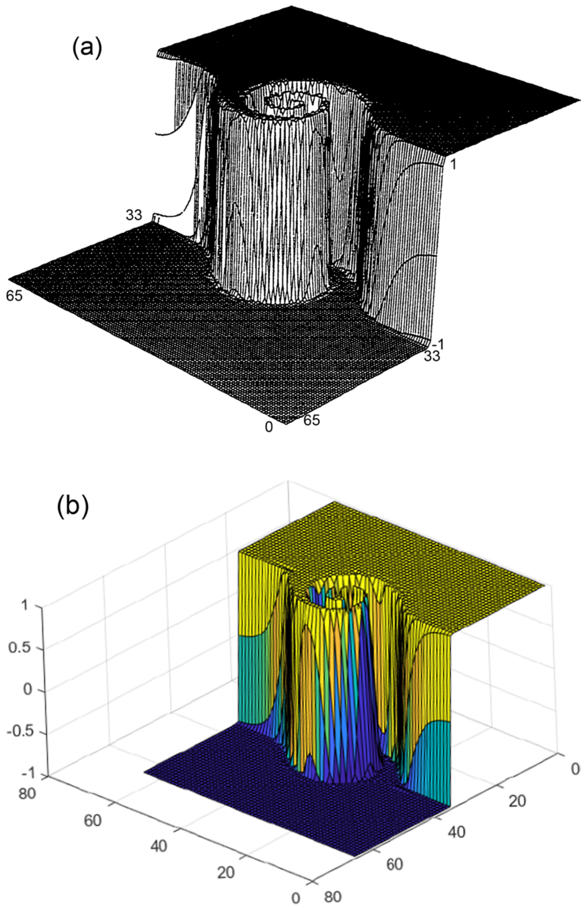

Fig. 3 Numerical simulation after 5-time units on 65 × 65 grids, δ = 0.05, and CLF = 4: **a** simulation from Complete version of SY(Error = 0.068), **b** simulation from current Economic model (Error = 0.147)

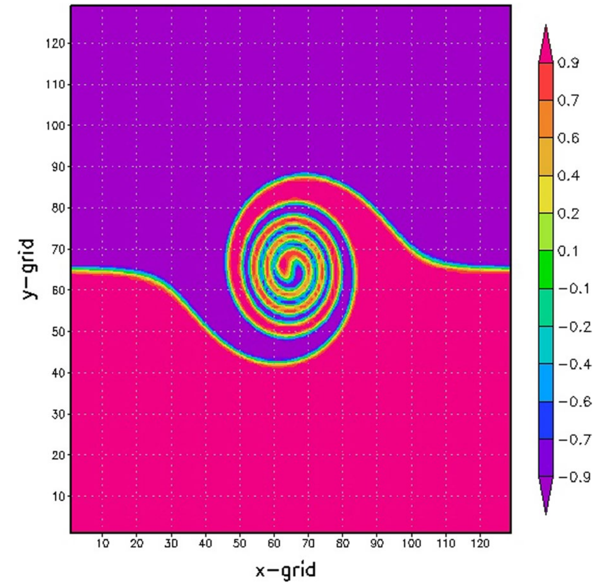

Fig. 4 Numerical simulation after 9.84-time units on 129 × 129 grids, δ = 0.05, and CLF = 6 (Error = 0.132) from current Economic model

is also well conserved (Error of mass is 6.176×10^{-4} at t = 9.843) by using Sun (2007), and Sun and Sun (2004). Because of simplicity and efficiency of the model, the current model is suitable to simulate the multi-dimensional fast-moving flows or to ease the constrained by unwanted acoustic waves in compressible fluid or gravity waves in simulating the flows in the atmosphere or oceans. It can be applied to predict the transport of pollutants and dust along the jet (Sun et al. 2013; Wu et al. 2003) and the high-speed raindrops falling from convective clouds (Sun 1993), or strong downslope windstorms in a three-dimensional complex terrain model (Haines et al. 2019; Sun and Sun 2015; Sun 2021) because of simplicity and accuracy. This scheme can also incorporate the variation method to ensure the conservation of mass and/or energy of the entire domain (Sun and Sun 2004; Sun 2007).

4 Conclusion

Here, we propose an efficient forward trajectory model, in which the property and position of the fluids can be accurately evaluated from the Euler coordinates advected to the Lagrangian coordinates. After sorting those fluid elements on the irregular Lagrangian curve, we apply the 3rd-order cubic polynomial to interpolate the coordinates and properties of the elements from the irregular curves to the regular grids. This scheme retains the advantages of the Internet Interpolation Model (SY) to allow a larger Courant number, but no need to solve the cubic equations and coefficients of a set of linear algebra equations as proposed by SY. The scheme is not only much simpler than SY's models but also allows using higher-degree polynomials. Hence, it is suitable to simulate the multiple-dimensional fast-moving flows in hurricanes, tornados and jet-streams, storms, and jet-stream, or ease the CFL constraint imposed by the unwanted acoustic waves in a compressible fluid or gravity waves in simulating the flow in the atmosphere and ocean (Mesinger and Arakawa 1976; Haltiner and Williams 1980; Lin 2007; Coiffier 2011; Lin et al. 2018). The semi-Lagrangian method can also avoid the nonlinear instability and is easier to handle the open lateral boundary compared with the finite difference and finite volume as discussed on p. 89 and p. 142 in the review article of Sun (2023).

Acknowledgements
The computing facility provided by Prof. P. L. Lin and Prof. C.Y. Huang at National Central University (NCU) is appreciated. Prof. Sun also sincerely thanks Profs. G. Lin and C. Huang for their help and discussions, and Prof. J. Y. Yu and reviewers for their comments, as well as the support from National Science and Technology Council, Taiwan for the author to visit NCU. The author withdrew this paper at the final gallery proof from Open Journal of Fluid Dynamics (OJFD) in March 2023 because OJFD broke the agreement and refused to include Taiwan in author's affiliation and Acknowledgements.

Author contribution
Dr. Sun has solely developed the numerical method and the computer programs.

Declaration

Competing interests
The author declares that there is no competing interest.

Received: 18 October 2023 Accepted: 5 January 2024
Published online: 17 January 2024

References

Coiffier J (2011) Fundamentals of numerical weather prediction. Cambridge Press, New York, p 337
Doswell CA (1984) A kinematic analysis associated with a nondivergent vortex. J Atmos Sci 41:1242–1248. https://doi.org/10.1175/1520-0469(1984)041%3c1242:AKAOFA%3e2.0.CO;2
Fournier A (2005) Inverse problems in meteorology and seismology. In: Applied Math. Colloquium at CU Boulder. 2015/4/10, pp. 1–16. https://doi.org/10.13140/RG.2.1.4136.8087
Fujita TT (1974) Jumbo Tornado Outbreak of 3 April 1974. Weatherwise 27(3):116–126
Fujita TT (1992) Memoris of an effort to unlock the mystery of severe storms: during the 50 years, 1942-1992. Wind Research Laboratory, Dept. of Geophysical Sciences, University of Chicago, p 298 (WRL research paper; no 239, Classifications: Dewey Decimal 551.55, Library of Congress QC943.5.U6 F85 1992)
Haines P, Sun WY, Chen SH, Hsu WR, Hsieh ME (2019) NTU/PU model simulations and observed flow over mountain. Terr Atmos Ocean Sci 30:171–184. https://doi.org/10.3319/TAO.2018.12.04.01
Haltiner GJ, Williams RT (1980) Numerical prediction and dynamic meteorology, 2nd edn. Wiley, Hoboken, p 477
Holm EV (1995) A fully two-dimensional, no oscillatory advection scheme for momentum and scalar transport equations. Mon Weather Rev 123:536–552. https://doi.org/10.1175/1520-0493(1995)123%3c0536:AFTDNA%3e2.0.CO;2
Hsieh M-N, Hsu W-R, Sun W-Y (2010) Applications of a three-dimensional nonhydrostatic atmospheric model on uniform flows over an idealized mountain. In: The 17th National Computational Fluid Dynamics Conference, Taoyuan, 29–31 July 2010. pp. 1–7
Hsu W-R, Hou JP, Wu CC, Sun WY, Tcheng SC, Chang HY (2004) Large-eddy simulation of cloud streets over the East China Sea during cold-air outbreak events. In: 16th Symposium on Boundary Layers and Turbulence, Portland, Maine, 9–13 August 2004. pm.2.4. pp. 1–7
Kalnay E, Park SK, Pu ZX, Gao J (2000) Application of the quasi-inverse method to data assimilation. Mon Wea Rev 128(3):864–875. https://doi.org/10.1175/1520-0493(2000)128%3c0864:AOTQIM%3e2.0.CO;2
Kurihara Y, Tuleya RE, Bender MA (1998) The GFDL hurricane prediction system and its performance in the 1995 hurricane season. Mon Wea Rev 126:1306–1322. https://doi.org/10.1175/1520-0493(1998)126%3c1306:TGHPSA%3e2.0.CO;2
Lin YL (2007) Mesoscale dynamics. Cambridge University Press, New York, p 633
Lin M-Y, Sun WY, Chiou M-D, Chen C-Y, Cheng H-Y, Chen C-H (2018) Development and evaluation of a storm surge warning system in Taiwan. Ocean Dyn 68:1025–1049. https://doi.org/10.1007/s10236-018-1179-z
Mesinger F, Arakawa A (1976) Numerical methods used in atmospheric models. GARP Glob Atmos Res Program 17:64
Nair RD, Scroggs JS, Semazzi FHM (2003) A forward-trajectory global semi-Lagrangian transport scheme. J Comput Phys 190:275–294. https://doi.org/10.1016/S0021-9991(03)00274-2
Purser RJ, Leslie LM (1991) An efficient interpolation procedure for high-order three- dimensional semi-Lagrangian models. Mon Weather Rev 119:2492–2498
Purser RJ, Leslie LM (1994) An efficient semi-Lagrangian scheme using third-order semi-implicit time integration and forward trajectories. Mon Weather Rev 122:745–756. https://doi.org/10.1175/1520-0493(1991)119%3c2492:AEIPFH%3e2.0.CO;2
Riehl H, Malkus JS (1958) On the heat balance in the equatorial trough zone. Gephysica 6:503–538
Seitter KL, Kuo HL (1983) Dynamical structure of squall-line type thunderstorms. J Atmos Sci 40:2831–2854
Staniforth A, Cote J (1991) Semi-Lagrangian integration schemes for atmospheric models- a review. Mon Weather Rev 119:2206–2223. https://doi.org/10.1175/1520-0493(1991)119%3c2206:SLISFA%3e2.0.CO;2
Sun WY (1993) Numerical simulation of a planetary boundary layer: Part II. Cloudy case. Beitrage Zur Physik Der Atmos 66:17–30
Sun WY (2007) Conserved Semi-Lagrangian scheme applied to one-dimensional shallow water equations. Terr Atmos Ocean Sci 18(4):777–803. https://doi.org/10.3319/TAO.2007.18.4.777(A)
Sun WY (2011) Instability in leapfrog and forward-backward schemes: Part II: Numerical simulation of dam break. J Comput Fluids 45:70–76. https://doi.org/10.1016/j.compfluid.2010.11.002
Sun WY (2021) Coordinates over complex terrain in atmospheric model. J Atmos Sci Res. https://doi.org/10.30564/jasr.v4i1.2704
Sun WY (2023) Challenges and progress in computational geofluid dynamics in recent decades. Atmosphere 14(1324):1–149. https://doi.org/10.3390/atmos14091324
Sun WY, Oh TJ (2022) Vortex merger in shallow water model. Asia-Pac J Atmos Sci. https://doi.org/10.1007/s13143-022-00270-9
Sun WY, Sun MT (2004) Mass correction applied to semi-Lagrangian advection scheme. Mon Wea Rev 132(4):975–984
Sun WY, Sun OM (2015) Bernoulli equation and flow over a mountain. Geosci Lett 2:7. https://doi.org/10.1186/s40562-015-0024-1
Sun WY, Sun OM (2017) Backward integration of diffusion. Aerosol Air Qual Res 17:278–289. https://doi.org/10.4209/aaqr.2016.06.2071
Sun WY, Sun OM (2019) Revisiting the parcel method and CAPE. Dyn Atmos Oceans 86:134–152. https://doi.org/10.1016/j.dynatmoce.2019.03.008
Sun WY, Yeh K-S (1997) A general semi-Lagrangian advection scheme employing forward trajectories. Q J R Meteorol Soc 123:2463–2476. https://doi.org/10.1002/qj.49712354415
Sun WY, Yeh K-S, Sun RY (1996) A simple semi-Lagrangian scheme for advection equations. Q J R Meteorol Soc 122:1211–1226. https://doi.org/10.1002/qj.49712253310
Sun WY, Yang KJ-S, Lin N-H (2013) Numerical simulations of Asian dust-aerosols and regional impacts on weather and climate—Part II: PRCM-dust model simulation. Aerosol Air Qual Res 13:1641–1654. https://doi.org/10.4209/aaqr.2013.06.0208
Toro EF (1999) Riemann solvers and numerical methods for fluid dynamics. Springer, Berlin, p 309. https://doi.org/10.1007/978-3-662-03915-1
Wang H, Yeh GT (2005) A characteristic-based semi-Lagrangian method for hyperbolic systems of conservation laws. Chin J Atmos Sci 29:21–42
Wu CC, Yu YC, Hsu WR, Hsu KJ, Sun WY (2003) Numerical study on the wind fields and atmospheric transports of a typical winter case in Taiwan and surrounding area. Atmos Sci 31(大氣科學; 31卷1期):29–54
Yeh KS, Cote J, Gravel S, Methot A, Patoine A, Roch M, Staniforth A (2002) The CMC–MRB global environmental multiscale (GEM) model. Part III: nonhydrostatic formulation. Mon Wea Rev 130:339–356

Publisher's Note